Chemical generation of checkpoint inhibitory T cell engagers (CiTEs) for the treatment of cancer

Peter A. Szijj,[a] Melissa A. Gray,[b,†] Mikaela K. Ribi,[b,†] Calise Bahou,[a] João C. F. Nogueira,[a] Carolyn R. Bertozzi,[b*] Vijay Chudasama[a*]

a: Department of Chemistry, University College London, 20 Gordon Street, London, WC1H 0AJ, UK. E-mail: v.chudasama@ucl.ac.uk

b: Department of Chemistry, Sarafan ChEM-H, and Howard Hughes Medical Institute, Stanford University, Stanford, CA, E-mail: bertozzi@stanford.edu

*: Correspondence: v.chudasama@ucl.ac.uk, bertozzi@stanford.edu

†: These authors contributed equally to this work.

Graphical Abstract

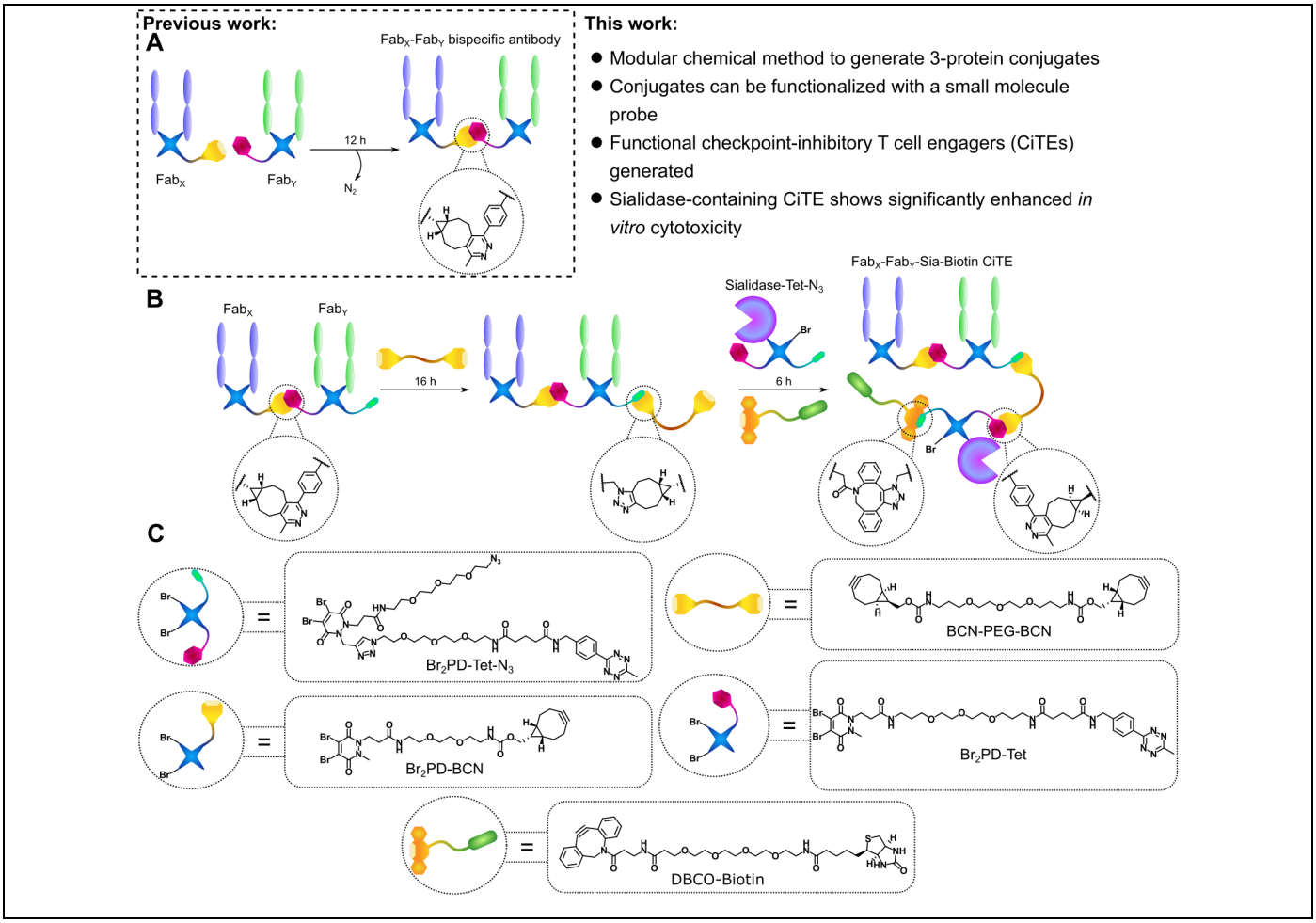

Abstract

Bispecific antibodies (bsAbs) provide enticing therapeutic opportunities in the area of immunotherapy, especially in the field of immuno-oncology. These constructs can bind two separate antigenic epitopes and thus provide access to unique mechanisms of action (MoAs). A key MoA is unlocked by bispecific T cell engagers (BiTEs), which cause T cells to be cross-linked with a targeted cancer cell, ultimately leading to death of the targeted cell. It has been shown that the combination of a BiTE with checkpoint inhibition, such as blockade of the PD-1/PD-L1 pathway, can lead to a synergistic effect and greater efficacy. Constructs built from a BiTE core (anti-CD3/anti-cancer antigen) with an immunomodulatory protein added, have been dubbed checkpoint-inhibitory T cell-engagers (CiTEs). Both bsAbs and CiTEs have traditionally been generated *via* protein engineering. However, recently, improved chemical methods for the construction of bsAbs have been reported. This includes a strategy developed by the Chudasama and Baker groups to synthesize homogenous fragment-based bsAbs from antibodies' fragments antigen binding (Fabs), utilising click-enabled pyridazinediones (PDs) for functional disulfide re-bridging, followed by strain-promoted inverse electron-demand Diels-Alder cycloaddition (SPIEDAC) click chemistry to attach the two Fabs to each other. In this paper, we describe a first-in-class chemical method to generate biotin-functionalized three-protein conjugates, building significantly on the previously described PD-method. The three-protein constructs generated here include two such CiTE molecules, one containing an anti-PD-1 Fab, the other containing an immunomodulatory enzyme *Salmonella typhimurium* sialidase; Fab_{CD3}-Fab_{HER2}-$Fab_{PD\text{-}1}$-Biotin and Fab_{HER2}-Fab_{CD3}-Sia-Biotin. These constructs (along with suitable controls) were tested for their biological activity, and each of their protein components were shown to retain their function. Their efficacy was also compared to a simpler BiTE scaffold and was shown to be superior, with the sialidase-containing CiTE especially showing significantly enhanced potency *in vitro*. The chemical method described here has the potential to enable the rapid generation of a plethora of multi-protein constructs, which we envisage would be especially useful in hit-identification screening but could also potentially be scaled up for drug-development after further optimization.

Recently, the field of bispecific antibodies (bsAbs) has been garnering increased interest and momentum with there now being five such therapeutics on the market, of which three have been approved by the FDA or EMA within the past year.[1,2] This class of (primarily) artificial protein-constructs are characterized by the capacity to simultaneously bind to two distinct antigenic epitopes, be they on the same or different target biomacromolecules. This dual-binding facilitates novel mechanisms of action (MoAs) that are unavailable to traditional monospecific antibodies.[3] However, the full potential for protein–protein conjugation is yet to be unlocked, as even more advanced MoAs can be accessed through the generation of multi-protein conjugates, especially with the option to attach small molecule functionalities. A promising class of such molecules combines T cell re-directing bsAb technology with immunomodulating proteins for additional therapeutic benefit.[4] Here we report a first-in-class chemical method for the synthesis of functionalized three-protein conjugates and then test their efficacy *in vitro*.

1. Chemical bispecific antibody-generation

To appreciate the challenges that need to be overcome to access three-protein conjugates, an understanding of the methods for bsAb generation is required. The standard strategy of producing bsAb constructs has to date relied on genetic/protein engineering to generate fused amino-acid sequences, which can then be expressed. However, the field of protein bioconjugation (i.e., how to attach small molecules to proteins) has undergone rapid advances in the past decade, leading to the recent emergence of new chemical methods for bsAb production. These improved chemistry-based strategies can offer benefits over expression-based methods as they conceptually offer greater modularity, speed, and potentially inherent handles for further functionalization, e.g., for the generation of bispecific antibody-drug or fluorophore conjugates. For a more comprehensive overview of the subject of chemical bsAb-synthesis, the readers are referred to two recent reviews on the topic.[5,6]

The most modern purely chemical approaches for site-selective homogeneous bsAb formation rely on re-bridging the solvent accessible interchain disulfide bonds of antibodies or their antigen-binding fragments (Fabs). As the natural abundance of cysteine is low[7] and most antibodies contain only four readily accessible disulfides, with Fabs containing only one, site-selective modification of these proteins can be achieved in this way. Homogeneous and well-defined bsAbs can only be generated through such site-selective functionalization strategies – as any heterogenous conjugation strategy would by definition lead to a heterogenous bsAb.

The first example of a chemically produced Fab-Fab conjugate was published in 2013, where two bis-sulfone molecules attached to a large PEG linker were used to generate a monospecific Fab-PEG-Fab construct.[8] Subsequently, maleimide molecules with leaving groups on each double bond (termed “next-generation maleimides”, NGMs) were attached to each other to generate bis-NGM molecules. These were

used to synthesize a range of constructs; e.g., Fab-ScFv and albumin-Fab heterodimers and an $(ScFv)_3$ homotrimer.[9,10] A more modular strategy was reported combining the site-selective modification provided by the NGM platform and the flexibility of strain-promoted azide-alkyne cycloaddition (SPAAC) click chemistry to generate Fab-Fab[11] and full length IgG2-IgG2 bispecific antibodies.[12] While these methods showed promise, they were limited by long reaction times, poor yields and the inability to functionalise the constructs further.

The Chudasama and Baker groups, however, recently developed a rapid and modular click-chemistry-based method for the construction of homogeneous bispecific antibody-conjugates, with the ability to add additional functionality to the bsAb.[13] These attributes were key in the search for a chemical method applicable to the synthesis of three-protein conjugates. The method was based on the dibromopyridazinedione scaffold[14–18] which was employed to re-bridge the disulfide bonds of enzymatically generated (or expressed) Fabs to functionalize the protein with bioorthogonal click handles, strained alkyne and tetrazine. These click-enabled Fabs could react with each other *via* strain-promoted inverse electron-demand Diels-Alder cycloaddition (SPIEDAC) reaction to generate a bsAb construct where the two proteins are linked by a flexible PEG-containing tether. As pyridazinediones contain two *N*-atoms in the ring, a second functional handle could be introduced. This was demonstrated with the attachment of two distinct fluorescent dyes to the bsAb *via* Cu-catalysed azide/alkyne click.[13] However, due to the toxicity associated with Cu, and difficulties with its removal, in line with recent trends in bioorthogonal chemistry, it was thought that the method could be improved by having both click reactions be Cu-free. In this manner, the final Cu-free click could be used to introduce a 3rd protein to generate a three-protein conjugate.

The primary objective of this work was the development of a chemical method for three-protein conjugate synthesis. This work thus explored the Cu-free chemical construction of functionalised bsAbs, followed by the generation of bsAb-enzyme and trispecific antibody (tsAb) conjugates. To date, to the best of our knowledge, no complexes composed of three different proteins have been assembled *via* chemical means. Going a step further, further functionalization of these constructs with a biotin molecule to assist in applications (such as imaging) and purification was attempted. Finally, to showcase the functionality of these constructs, and to demonstrate that a key characteristic of the method described herein is its modularity, functional molecules were generated, the biological activities of which were then explored.

2. Checkpoint-inhibitory T cell engagers (CiTEs)

The class of functional molecules synthesized here can be termed “checkpoint-inhibitory T cell engagers” (CiTEs).[19] These combine the cytotoxic ability of bispecific T cell engagers (BiTEs)[20,21] with a checkpoint inhibitory modality to further enhance T cell activation and thus efficacy. Limited examples of such three-protein or four-protein conjugates, all generated *via* protein engineering, have been reported in the

context of immunotherapy – these have been reviewed recently.[4] For the purposes of this work, formats where T cell engagement are combined with immunomodulation should be discussed in more detail.

In the field of T cell redirection it has been shown that blockade of the PD-1/PD-L1 immune checkpoint axis could reverse immune escape in primary acute myeloid leukaemia (AML) cells *ex vivo* on treatment with an anti-CD33 BiTE.[22] While the AML cells did not constitutively express PD-1, the expression of the protein was upregulated on addition of BiTE, due to pro-inflammatory cytokine release. Addition of anti-PD-1 or anti-PD-L1 antibody increased the cytotoxic ability of the BiTE. Based on these observations, Herrmann *et al.* have reported the generation of an anti-CD33/anti-CD3/PD-1_{ex} construct, comprising the fusion of an anti-CD33 and an anti-CD3 scFv with the low affinity extracellular region of PD-1, thus combining an anti-CD33 BiTE with blockade of the PD-1/PD-L1 immune checkpoint.[19] The authors of the work dubbed this molecule a checkpoint inhibitory T-cell engager (CiTE). The affinity of the PD-L1 binding moiety, the PD-1_{ex} in this case, was kept low to stop the CiTE from exhibiting systemic checkpoint blockade, and only do so in a targeted manner on AML cells, as directed by the anti-CD33 arm. This was hoped to reduce the adverse effects associated with systemic checkpoint blockade, and also to stop the CiTE from localizing to off-cancer cells thus reducing on-cancer efficacy. A similar anti-CD33/anti-CD3/anti-PD-L1 species, constructed previously from three scFv proteins *via* fusion, dubbed a single-chain triplebody (sctb), served as a high affinity control, as the anti-PD-L1 scFv had a high affinity for PD-L1.[23] The CiTE was shown to only induce lysis of $CD33^{+}$PD-$L1^{+}$ AML cells *in vitro*, whereas $CD33^{-}$PD-$L1^{+}$ non-AML cells were not affected. The CiTE was also shown to not lead to on-target off-cancer events as measured by lack of murine body weight loss and lack of systemic T cell activation, as seen by a lack of PD-1 upregulation. The sctb on the other hand was also able to kill $CD33^{-}$PD-$L1^{+}$ cells in addition to $CD33^{+}$PD-$L1^{+}$ cells, caused murine body weight loss, and systemic PD-1 upregulation.[19] This study provided an elegant and promising new strategy for combining checkpoint blockade with immune cell redirection.

Of note is that neither of the three-protein conjugate platforms discussed here (CiTE[19] or sctb[23]) has an Fc fragment or similar half-life extending functionality incorporated. Thus, carefully monitoring the pharmacokinetics, and potentially considering half-life extension technologies may be required. These methods could also benefit from the increased flexibility that could potentially be offered by chemical methods for the generation of three-protein conjugates. Even from such a brief showcase, it is clear that the pool of protein components from which these species can be constructed is vast, and many parameters have to be considered (e.g., cancer target, binding-affinities, immune checkpoint pathway to modulate, potential side-effect caused by immune cell activation, half-life, tumour penetration, Fc-mediated effector function or lack thereof). The addition of small molecules to either modulate function, provide theranostic capabilities, or just as tools to allow for monitoring of the biodistribution of these species may also provide benefit. It follows that a modular method which can rapidly produce conjugates from a pool of components for initial testing would be advantageous.[4]

The CiTEs envisaged here have an anti-CD3/anti-HER2 core with a checkpoint inhibitory Fab (anti-PD-1 Fab) or a checkpoint modulating enzyme (*Salmonella typhimurium* Sialidase, ST Sia) attached. To understand the significance of ST Sia, the role of sialic acid in immune regulation will be briefly examined. An important immune dampening signal of healthy cells comes from cell surface glycans terminating in sialic acid. These can bind the sialic acid-binding Ig-like lectins (Siglecs) on the surface of immune cells to downregulate the immune response. Unfortunately, cancer cells have evolved to exploit this mechanism by overexpressing sialic acid to evade detection and destruction by immune cells. The Bertozzi group have shown that fusing a sialidase moiety, which removes sialic acid from cell-surface glycans, to the anti-HER2 antibody trastuzumab can significantly increase antibody-dependent cellular cytotoxicity (ADCC) and natural killer (NK) cell-mediated killing in cells that express lower amounts of HER2, and would thus be resistant to trastuzumab monotherapy.[24] Subsequently, this strategy was expanded on, first by identifying an optimal sialidase enzyme for the conjugate. It was shown that using an enzyme with low intrinsic binding affinity would minimize off-target, antibody-independent, effects. On expressing and testing 6 different sialidases, the enzyme from *Salmonella typhimurium* (ST) was found to be the optimal candidate and was indeed shown to improve the therapeutic window 33-fold over the originally used *Vibrio cholerae* (VC) sialidase in a co-culture assay of a $HER2^+$ and $HER2^-$ cell line. To improve stability of the conjugate, a mutant ST sialidase with a C-terminal cysteine was expressed. This residue was selectively modified (over the 4 endogenous cysteines) with an α-chloroacetamide-DBCO molecule to insert a strained-alkyne click-handle. Trastuzumab functionalized with an azide functionality was also prepared *via* a hydrazino-iso-Pictet Spengler (HIPS) reaction. The ST sialidase-DBCO moiety was then clicked to trastuzumab-N_3 *via* strain-promoted azide-alkyne cycloaddition (SPAAC), to produce the optimized trastuzumab-sialidase (Ab_{HER2}-Sia) conjugate. It was also shown, that having one sialidase per antibody increased on-target enzymatic activity, while it was theorized that the reduced number of enzymes would also reduce off-target activity. With these results in hand, the Ab_{HER2}-Sia construct was tested on a $HER2^+$, but trastuzumab resistant, mouse tumour model. Ab_{HER2}-Sia was shown to delay tumour growth when compared to trastuzumab alone.[25] Of additional note is a study that has been recently published outlining the mechanism of involvement of sialic acid in the regulation of the CD28 – CD80/CD86 costimulatory pathway.[26] This pathway is required alongside the antigen recognition mediated by the TCR/MHC axis for the differentiation of naïve T cells into functional effector T cells. It was shown that sialic acids are alternative ligands for CD28, thus blocking the binding of CD28 to CD80/CD86 and inhibiting T cell activation. Enzymatic removal of sialic acids from either T cells or antigen presenting cells can rescue T cell activation. Additionally, it was shown that exhausted, hypofunctional $PD\text{-}1^+$ T cells can be revived by treatment with sialidase enzyme.

Thus, it was envisioned, that combining the ability of a sialidase enzyme, or a PD-1/PD-L1 checkpoint inhibitor, to remove one of a cancer cell's mechanisms for immune escape, and its capability to re-invigorate exhausted T cells with the potency of bispecific T-cell engagers (BiTEs)[21] in killing target cells, a potent therapeutic could be constructed.

Multiple methods were trialled to generate the desired three-protein CiTEs. The initial strategy, relying on the conversion of a bsAb-N_3 into a bsAb-$PDBr_2$ through SPAAC click with a bicyclononyne (BCN) strained alkyne-functionalized PD molecule, followed by addition of reduced Fab or ST sialidase (expressed with an SLCTPSRGS amino acid sequence at the C-terminus to introduce a solvent-accessible cysteine)[25] to react with the PD molecule on the bsAb, met with some success. It was, however, hard to reproduce due to competing side-reactions which made the process less reliable (for detailed information, see ESI). The subsequently developed method, which will be detailed here, relied on strain-promoted inverse electron-demand Diels-Alder cycloaddition (SPIEDAC) reaction between tetrazine and BCN strained alkyne to achieve all protein–protein linkages. As this reaction was shown to work well for bispecific formation previously,[13] it was envisaged that it would be optimal for the installation of the third protein (sialidase **1** or $Fab_{PD\text{-}1}$ **2**).

The plan thus involved initially generating a bispecific Fab-Fab construct bearing an azide handle. This Fab_X-Fab_Y-N_3 construct would then be converted to Fab_X-Fab_Y-BCN *via* reaction with BCN-PEG-BCN (in 10-fold excess to limit cross-linking). This Fab_X-Fab_Y-BCN could then be reacted with Sia-Tet-N_3 **3** or $Fab_{PD\text{-}1}$-Tet-N_3 **4** and DBCO-Biotin **5** *in situ*, to add the enzyme or 3rd Fab (*via* tetrazine–BCN click), and a biotin molecule (*via* azide–DBCO click) to further aid in purification or imaging (see Graphical Abstract).

Initially, Fab_{HER2}-BCN **6** was reacted sequentially in a one-pot reaction with Sia-Tet-N_3 **3** and DBCO-Biotin **5** (Figure 1/A) to assess the orthogonality of the tetrazine–BCN and DBCO–azide clicks, as well as to test the stability of the sialidase enzyme **1** under the reaction conditions. As the enzyme was previously found to be acid-sensitive, the click reaction was carried out at pH 7 (PBS) instead of pH 5 (acetate). The reaction proceeded well, generating Fab_{HER2}-Sia-Biotin **7** (Figure 1/F). After monomeric avidin agarose purification clean Fab_{HER2}-Sia-Biotin **7** was isolated, with the purity confirmed by LC-MS (Figure 1/K) and SDS-PAGE (Figure 1/F). Additionally, a Fab_{HER2}-Fab_{CD3}-Biotin **8** bispecific T cell engager (BiTE) bsAb was synthesized. Initially, Fab_{HER2}-Fab_{CD3}-N_3 bsAb **9** was constructed, then after SEC purification (Figure 1/E) this was reacted with DBCO-Biotin to yield the biotinylated construct Fab_{HER2}-Fab_{CD3}-Biotin **8** (Figure 1/C). The purity of the constructs was confirmed by SDS-PAGE (Figure 1/G) and LC-MS (Figure 1/I-J).

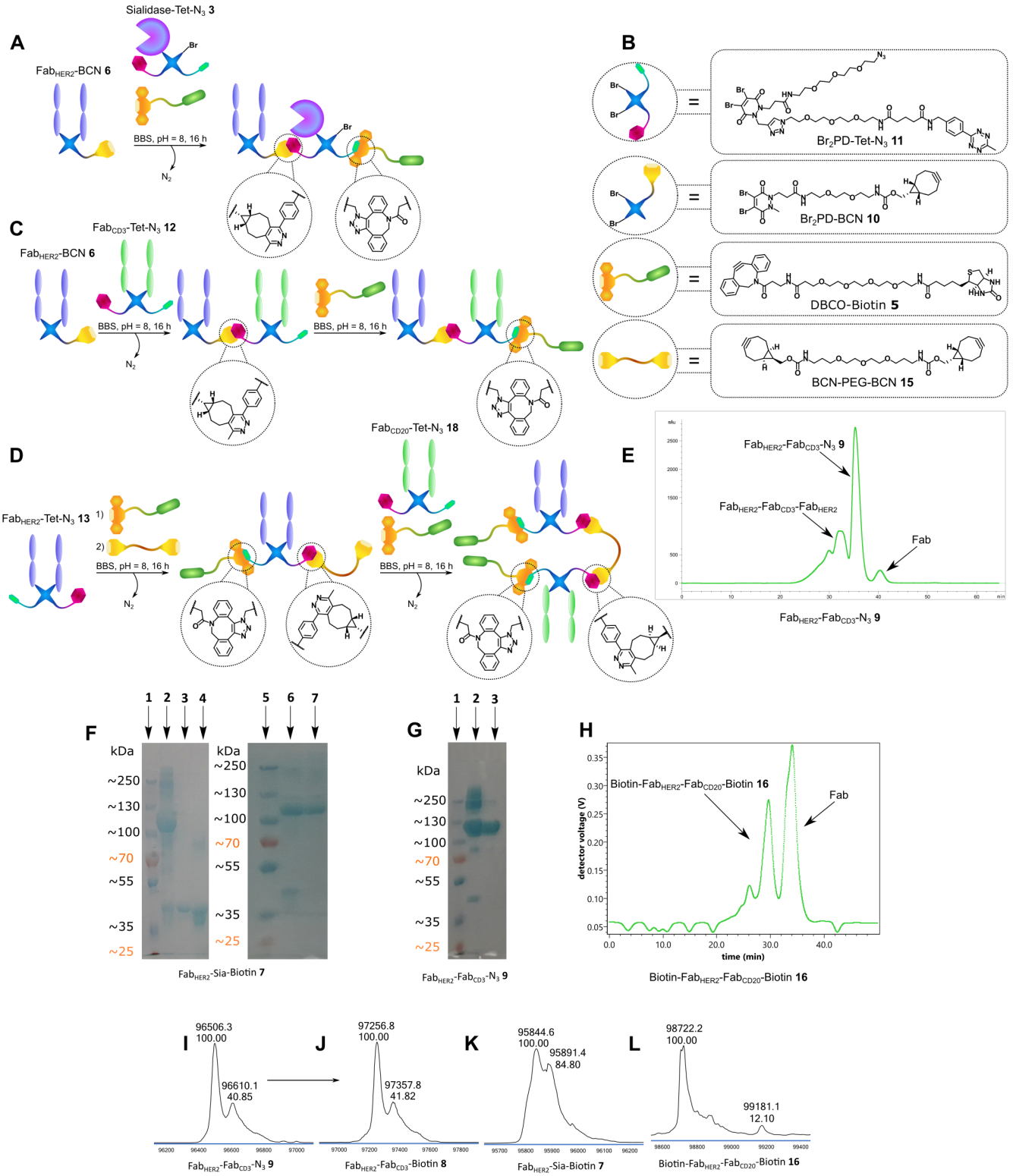

Figure 1 **| Generation of biotinylated bsAbs and the Fab_{HER2}-Sialidase conjugate 7 with pyridazinediones (PDs).**

A | Generation of Fab_{HER2}-Sia-Biotin **7**. Fab_{HER2}-BCN **6** was reacted with Sia-Tet-N_3 **3** and DBCO-Biotin **5** to generate Fab_{HER2}-Sia-Biotin **7** after monomeric avidin agarose purification. **B |** The PDs used for the generation of biotinylated bsAbs and Fab_{HER2}-Sia-Biotin **7**; Br_2PD-BCN **10** and Br_2PD-Tet-N_3 **11**. The BCN-PEG-BCN linker **15** used for the generation of a bis-biotinylated bsAb **16**. DBCO-Biotin **5** was used to biotinylate the constructs. **C** | Generation of Fab_{HER2}-Fab_{CD3}-Biotin **8**. Fab_{HER2}-BCN **6** was reacted with

Fab_{CD3}-Tet-N_3 **12** to form Fab_{HER2}-Fab_{CD3}-N_3 **9**. This construct was then reacted with DBCO-Biotin **5** to generate Fab_{HER2}-Fab_{CD3}-Biotin **8** after size-exclusion chromatography (SEC) purification. **D |** Generation of Fab_{HER2}-(Biotin)-Fab_{CD20}-Biotin **16**. Fab_{HER2}-Tet-N_3 **13** was reacted with DBCO-Biotin **5** for 1 h to afford Fab_{HER2}-Tet-Biotin **14**, followed by *in situ* addition of BCN-PEG-BCN **15** to generate Fab_{HER2}-(Biotin)-BCN **17** over a further 15 h. After removal of excess small molecule, this was reacted with Fab_{CD20}-Tet-N_3 **18** and DBCO-Biotin **5** *in situ* to Fab_{HER2}-(Biotin)-Fab_{CD20}-Biotin **16** after SEC purification. **E |** SEC UV-trace of Fab_{HER2}-Fab_{CD3}-N_3 **9** formation reaction. **F |** SDS-PAGE analysis of Fab_{HER2}-Sia-Biotin **7**. **Lane 1 & 5:** Ladder. **Lane 2:** Crude Fab_{HER2}-Sia-Biotin **7**. **Lane 3:** Fab_{HER2}. **Lane 4:** Sia-Tet-N_3 **3**. **Lane 6:** Non-bound fraction of monomeric avidin agarose purification. **Lane 7:** Bound fraction of purification; Fab_{HER2}-Sia-Biotin **7**. **G |** SDS-PAGE analysis of Fab_{HER2}-Fab_{CD3}-N_3 **9**. **Lane 1:** Ladder. **Lane 2:** Crude Fab_{HER2}-Fab_{CD3}-N_3 **9**. **Lane 3:** Purified Fab_{HER2}-Fab_{CD3}-N_3 **9**. **H |** SEC UV-trace of Fab_{HER2}-(Biotin)-Fab_{CD20}-Biotin **16** formation reaction. **I |** LC-MS analysis of Fab_{HER2}-Fab_{CD3}-N_3 **9**. Expected mass: 96496 Da. Observed mass: 96506 Da. **J |** LC-MS analysis of Fab_{HER2}-Fab_{CD3}-Biotin **8**. Expected mass: 97246 Da. Observed mass: 97257 Da. **K |** LC-MS analysis of Fab_{HER2}-Sia-Biotin **7**. Expected mass: 95873 Da. Observed mass: 95845 Da and 95891 Da (Δ = 46 Da, formic acid, MS adduct). **L |** LC-MS analysis of Fab_{HER2}-(Biotin)-Fab_{CD20}-Biotin **16**. Expected mass: 98734 Da. Observed mass: 98722 Da and 99181 Da (Biotin-Fab_{HER2}-Fab_{HER2}-Biotin **19**, expected mass: 99193 Da).

As the bsAb produced by this method had an azide handle, it had to be converted to either a tetrazine or BCN to enable a tetrazine–BCN click to install the final protein. In this way we could ensure that all protein–protein attachment steps would be driven by the extremely fast BCN–Tetrazine IEDDA click, shown to be the best reaction to overcome the steric hindrance that makes the coupling of such large molecules difficult.[27] To this end, BCN-PEG-BCN molecule **15** was synthesized (details in ESI) to enable the conversion of bsAb-N_3 into bsAb-BCN.

To test the BCN-PEG-BCN molecule **15** and attempt the construction of a dually modified bsAb with Cu-free click chemistry, the synthesis of Fab_{HER2}-(Biotin)-Fab_{CD20}-Biotin **16** was carried out (Figure 1/D). Fab_{HER2}-Tet-N_3 **13** was reacted with DBCO-Biotin followed by BCN-PEG-BCN **15** sequentially, to generate Fab_{HER2}-BCN-Biotin **17**. This was then further reacted with Fab_{CD20}-Tet-N_3 **18** and DBCO-Biotin **5** *in situ* to yield Fab_{HER2}-(Biotin)-Fab_{CD20}-Biotin **16** after SEC purification (Figure 1/H). The purity of the construct was assessed *via* LC-MS (Figure 1/L). About 10% Fab_{HER2}-(Biotin)-Fab_{HER2}-Biotin **19** impurity was observed stemming from unwanted dimerization during the BCN-PEG-BCN **15**-addition step of the reaction. This could be mitigated by further reducing the concentration of the reaction and increasing the equivalents of BCN-PEG-BCN **15**. Unfortunately, the solubility of BCN-PEG-BCN **15** in water was suboptimal, and thus required careful monitoring to ensure the compound did not precipitate out of solution. This is not a major limitation when low equivalents are sufficient, but in this case where controlling a competing side-reaction depends on a large excess of the molecule, it is a concern. Here, two biotin molecules were

installed into the construct, but as they were added at different stages, two distinct cargo molecules could just as easily have been added. Thus, a first-in-class method for the Cu-free dual modification of a chemically constructed bsAb was developed.

With these encouraging preliminary results obtained, the generation of a first-in-class Fab_{HER2}-Fab_{CD20}-Sia-biotin species **20** was attempted (Figure 2/A). SDS-PAGE analysis showed that the bsAb formation proceeded well and after Fab_{HER2}-Fab_{CD20}-N_3 **21** was reacted with BCN-PEG-BCN **15** (and excess small molecule removed after 6 h), Sia-Tet-N_3 **3** and DBCO-biotin **5** addition lead to consumption of Fab_{HER2}-Fab_{CD20}-BCN **22** and appearance of a larger band (Figure 2/C). Interestingly, vigorous denaturing conditions (95 °C, 5 min) were required to increase the resolution of the gel. SEC purification showed that >80% conversion to the Fab_{HER2}-Fab_{CD20}-Sia-biotin **20** construct was achieved (Figure 2/E), which was encouraging compared to the best previous conversion of <50% (as detailed in the ESI). SDS-PAGE (Figure 2/G) and LC-MS analysis (Figure 2/I) confirmed the purity of the sample.

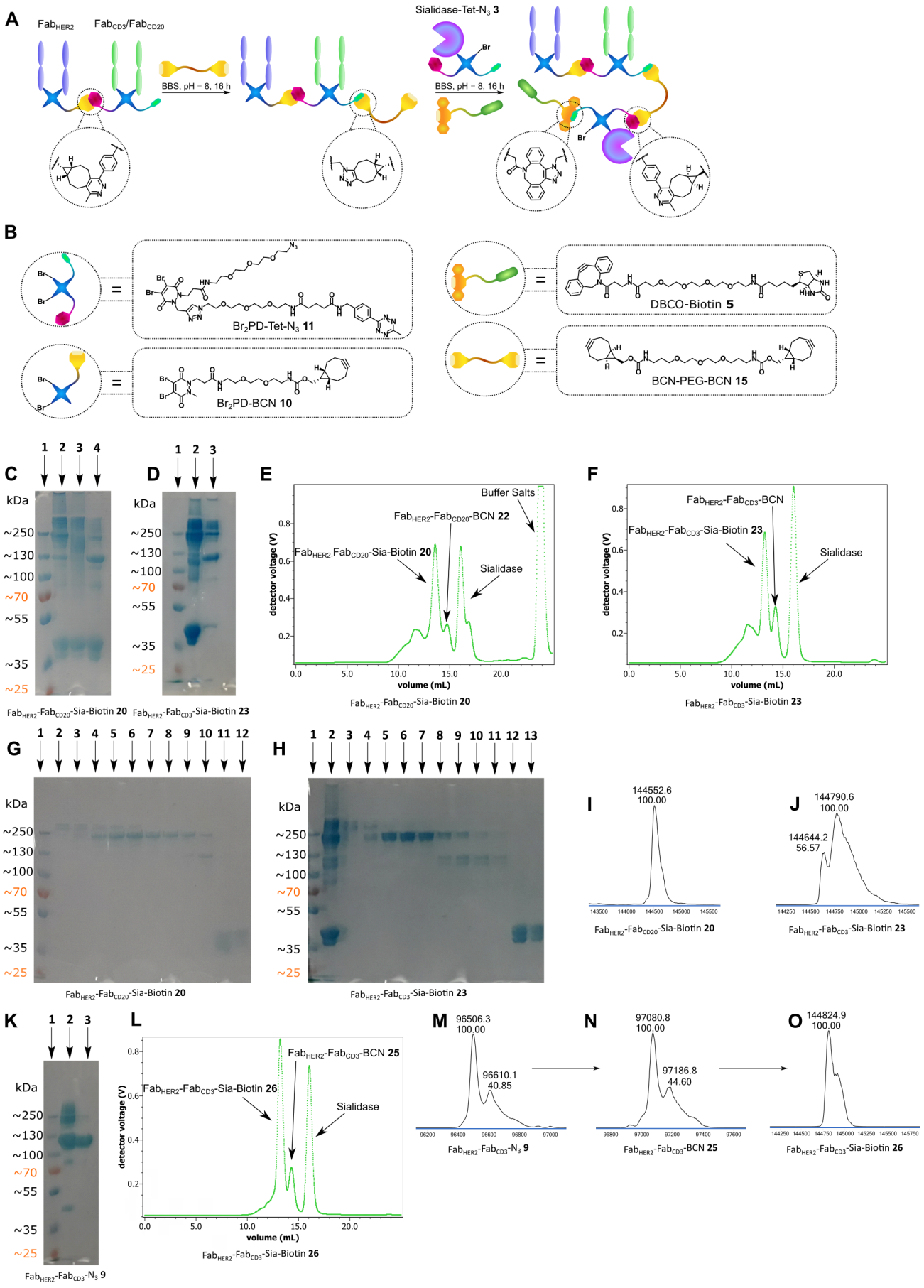

Figure 2 **| Synthesis of bsAb-Sia conjugates; Fab$_{HER2}$-Fab$_{CD20}$-Sia-Biotin 20 and Fab$_{HER2}$-Fab$_{CD3}$-Sia-Biotin CiTE 26.**

A | Method for the synthesis of bsAb-Sia conjugates. Fab_X-Fab_Y-N_3 is prepared as outlined before. This is then either SEC purified (for maximum final purity) or taken forward without purification to be reacted with BCN-PEG-BCN **15** to generate Fab_X-Fab_Y-BCN. Sia-Tet-N_3 **3** and DBCO-Biotin **5** are then added and reacted *in situ* to form Fab_X-Fab_Y-Sia-Biotin, which is then isolated after SEC purification. **B |** The PDs and small molecules used for the generation of bsAb-Sia-Biotin conjugates; Br_2PD-BCN **10**, Br_2PD-Tet-N_3 **11**, BCN-PEG-BCN linker **15** and DBCO-Biotin **5**. **C |** SDS-PAGE of Fab_{HER2}-Fab_{CD20}-Sia-Biotin **20** formation. **Lane 1:** Ladder. **Lane 2:** Fab_{HER2}-Fab_{CD20}-Sia-Biotin **20** heated at 95 °C for 5 min. **Lane 3:** Unheated Fab_{HER2}-Fab_{CD20}-Sia-Biotin **20**. **Lane 4:** Fab_{HER2}-Fab_{CD20}-N_3 **21** + Sia-Tet-N_3 **3** (no BCN-PEG-BCN **15** was added, thus no reaction was possible). **D |** SDS-PAGE of Fab_{HER2}-Fab_{CD3}-Sia-Biotin CiTE **23** formation. **Lane 1:** Ladder. **Lane 2:** Crude Fab_{HER2}-Fab_{CD3}-Sia-Biotin CiTE **23**. **Lane 3:** Crude Fab_{HER2}-Fab_{CD3}-N_3 **9**. **E |** UV trace of SEC purification of Fab_{HER2}-Fab_{CD20}-Sia-Biotin **20**. **F |** UV trace of SEC purification of Fab_{HER2}-Fab_{CD3}-Sia-Biotin CiTE **23**. **G |** SDS-PAGE of SEC purification of Fab_{HER2}-Fab_{CD20}-Sia-Biotin **20**. **Lane 1:** Ladder. **Lanes 2-3:** Aggregates. **Lanes 4-9:** Fab_{HER2}-Fab_{CD20}-Sia-Biotin **20**. **Lane 10:** Fab_{HER2}-Fab_{CD20}-BCN **22**. **Lanes 11-12:** Sia-Tet-N_3 **3**. **H |** SDS-PAGE of SEC purification of Fab_{HER2}-Fab_{CD3}-Sia-Biotin CiTE **23**. **Lane 1:** Ladder. **Lane 2:** Crude Fab_{HER2}-Fab_{CD3}-Sia-Biotin **23**. **Lane 3-4:** Aggregates. **Lanes 5-7:** Purified Fab_{HER2}-Fab_{CD3}-Sia-Biotin CiTE **23** (+ Fab_{HER2}-Fab_{CD3}-Fab_{HER2} **24** impurity). **Lanes 8-11:** Fab_{HER2}-Fab_{CD3}-N_3 **9**. Lanes **12-13:** Sia-Tet-N_3**3**. **I |** LC-MS analysis of Fab_{HER2}-Fab_{CD20}-Sia-Biotin **20**. Expected mass: 144532 Da. Observed mass: 144553 Da. **J |** LC-MS analysis of Fab_{HER2}-Fab_{CD3}-Sia-Biotin CiTE **23**. Expected mass: 144799 Da. Observed mass: 144791 and 144644 Da (Fab_{HER2}-Fab_{CD3}-Fab_{HER2} tsAb impurity, expected mass: 144632 Da). **K |** SDS-PAGE of SEC purification of Fab_{HER2}-Fab_{CD3}-N_3 **9**. **Lane 1:** Ladder. **Lane 2:** Crude Fab_{HER2}-Fab_{CD3}-N_3 **9**. **Lane 3:** Purified Fab_{HER2}-Fab_{CD3}-N_3 **9**. **L |** UV trace of SEC purification of Fab_{HER2}-Fab_{CD3}-Sia-Biotin CiTE **26** generated from SEC purified Fab_{HER2}-Fab_{CD3}-N_3 **9**. **M |** LC-MS analysis of Fab_{HER2}-Fab_{CD3}-N_3 **9**. Expected mass: 96493 Da. Observed mass: 96506 Da. **N |** LC-MS analysis of Fab_{HER2}-Fab_{CD3}-BCN **25**. Expected mass: 97065 Da. Observed mass: 97081 Da. **O |** LC-MS analysis of Fab_{HER2}-Fab_{CD3}-Sia-Biotin CiTE **26**. Expected mass: 144799 Da. Observed mass: 144825 Da.

Following these encouraging results, the generation of Fab_{HER2}-Fab_{CD3}-Sia-biotin **23** was attempted *via* the same strategy. Unfortunately, in this case, bispecific formation also led to a significant amount of undesired Fab_{HER2}-Fab_{CD3}-Fab_{HER2} trispecific antibody **24**, as shown by SDS-PAGE (Figure 2/D). Whilst not impacting further reactions, as it is of similar size as Fab_{HER2}-Fab_{CD3}-Sia-biotin **23**, SEC purification would not be able to separate them. As expected, addition of Sia-Tet-N_3 **3** and DBCO-biotin **5** lead to significant consumption of Fab_{HER2}-Fab_{CD3}-BCN **25** (Figure 2/D) and SEC purification confirmed good conversion (~70%) of bsAb to product **23** (Figure 2/F). SDS-PAGE (Figure 2/H) and LC-MS analysis (Figure 2/J) confirmed the purity of the sample, although with ~15% Fab_{HER2}-Fab_{CD3}-Fab_{HER2} **24** impurity arising from the bsAb-formation step of the reaction as discussed. This issue could be alleviated by either controlling the equivalents of Fabs to minimize the formation of trispecific antibody or scaling up the reaction and purifying the bsAb-N_3 **9** by SEC before subsequent reactions. Alternatively, a dual purification approach of

protein A and monomeric avidin agarose resin could be carried out, which should leave only species that contain both Fab_{HER2} (binds protein A) and Sia-biotin (binds avidin).

To address the purity issues of the final construct, the synthesis was repeated, this time with a purification after the bsAb-formation step. Fab_{HER2}-Fab_{CD3}-N_3 **9** was formed as before, albeit on a larger scale to account for mechanical protein-loss during purification, and subsequently purified by SEC (Figure 2/E). SDS-Page (Figure 2/G) and LC-MS analysis (Figure 2/I) confirmed the purity of the construct. A portion of the purified Fab_{HER2}-Fab_{CD3}-N_3 **9** was reacted with an excess of DBCO-Biotin **5** to yield Fab_{HER2}-Fab_{CD3}-Biotin **8**, the purity of which was confirmed by LC-MS (Figure 2/J).

The remainder of the Fab_{HER2}-Fab_{CD3}-N_3 **9** was treated with BCN-PEG-BCN **15** as before, over 6 h. After removal of excess small molecule the purity of the sample was confirmed by LC-MS (Figure 2/N) and then Sia-Tet-N_3 **3** and DBCO-Biotin **5** were added, and the mixture incubated for 20 h at 22 °C. After this time, the sample was SEC purified (Figure 2/L) and subsequently the purity was confirmed by LC-MS analysis (Figure 2/O). Gratifyingly, clean Fab_{HER2}-Fab_{CD3}-Sia-biotin **26** was obtained.

To further showcase the modularity of the three-protein conjugation approach developed here and to generate an additional useful construct, the synthesis of a Fab_{CD3}-Fab_{HER2}-$Fab_{PD\text{-}1}$-Biotin CiTE **27** was attempted (Figure 3/A). The synthesis of a Fab_{CD3}-Fab_{HER2}-N_3 bsAb **28** was carried out as before, although with the positions of the Fab_{CD3} and Fab_{HER2} arms swapped to showcase the modularity of the strategy and investigate the effect of Fab-placement within the construct on biological function. Following SEC purification (Figure 3/H), the purity of the construct was determined *via* SDS-PAGE (Figure 3/G) and LC-MS (Figure 3/C) analysis. The bsAb-N_3 **28** was converted to Fab_{CD3}-Fab_{HER2}-BCN **29** with BCN-PEG-BCN **15** as before (Figure 3/D). After removal of small molecule, $Fab_{PD\text{-}1}$-Tet-N_3 **4** (Figure 3/E) and DBCO-Biotin **5** were added to form Fab_{CD3}-Fab_{HER2}-$Fab_{PD\text{-}1}$-Biotin CiTE **27** after SEC purification (Figure 3/I). The purity of the construct was analysed *via* SDS-PAGE (Figure 3/G) and LC-MS (Figure 3/F). The SDS-PAGE analysis showed an additional fainter band beneath the main band, however the LC-MS spectrum showed only the expected masses (with the three major peaks arising from one-amino acid variations in the precursor Fabs as discussed in the ESI). We propose that this could be due to incomplete denaturation of the construct, with more completely denatured molecules traveling faster on the gel.

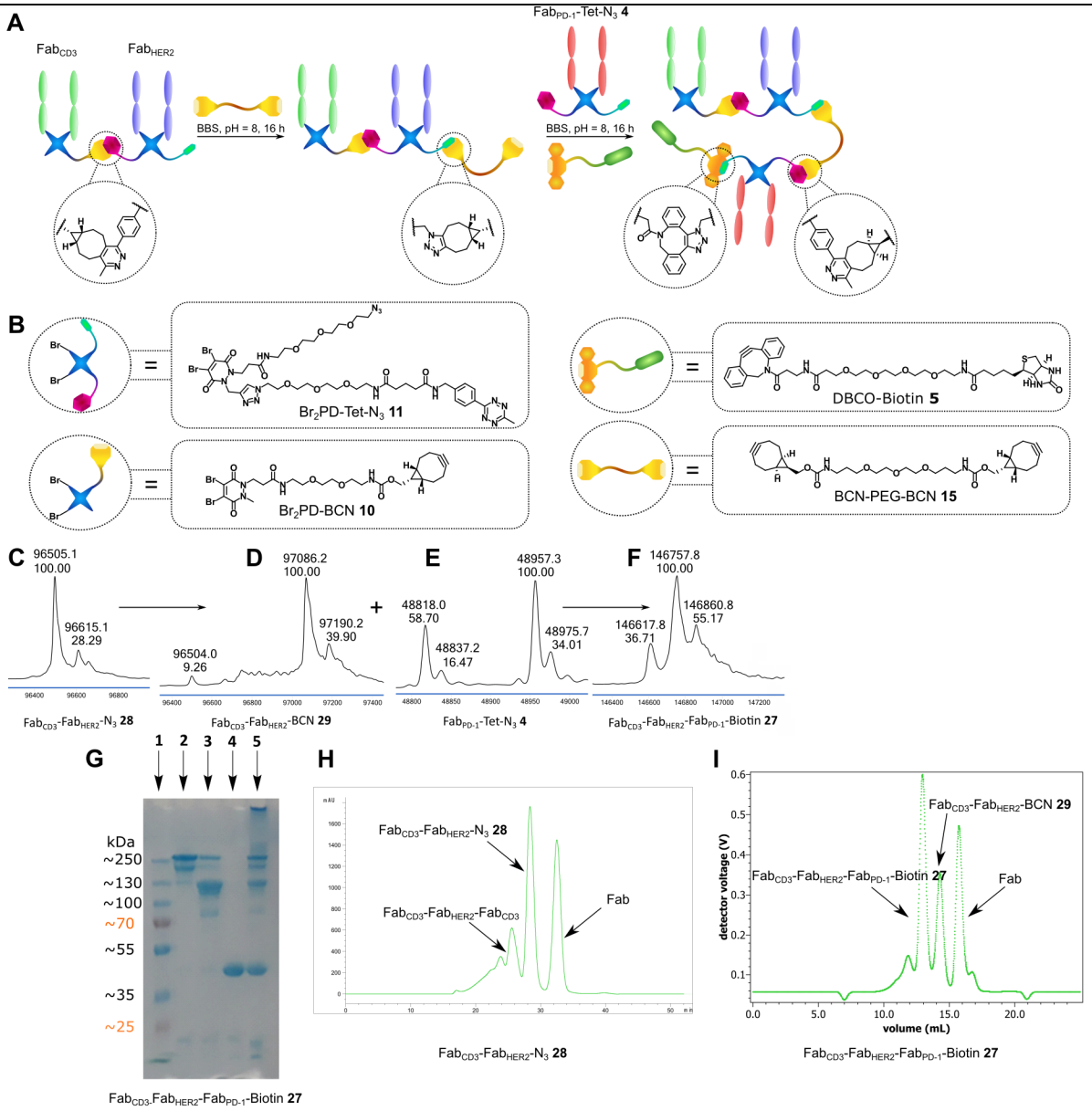

Figure 3 **| Synthesis of Fab$_{CD3}$-Fab$_{HER2}$-Fab$_{PD-1}$-Biotin CiTE 27.**

A | Method for the synthesis of Fab$_{CD3}$-Fab$_{HER2}$-Fab$_{PD-1}$-Biotin CiTE **27**. Fab$_{CD3}$-Fab$_{HER2}$-N$_3$ **28** was prepared as outlined before. This was then SEC purified and reacted with BCN-PEG-BCN **15** to generate Fab$_{CD3}$-Fab$_{HER2}$-BCN **29**. Fab$_{PD-1}$-Tet-N$_3$ **4** and DBCO-Biotin **5** were then added and reacted *in situ* to form Fab$_{CD3}$-Fab$_{HER2}$-Fab$_{PD-1}$-Biotin CiTE **27**, which was then isolated after SEC purification. **B |** The PDs and other small molecules used for the generation of CiTE conjugate **27**; Br$_2$PD-BCN **10**, Br$_2$PD-Tet-N$_3$ **11**, BCN-PEG-BCN linker **15**, and DBCO-Biotin **5**. **C |** LC-MS analysis of Fab$_{CD3}$-Fab$_{HER2}$-N$_3$ **28**. Expected mass: 96496 Da and 96610 Da. Observed mass: 96505 Da and 96615 Da. **D |** LC-MS analysis of Fab$_{CD3}$-Fab$_{HER2}$-BCN **29**. Expected mass: 97068 Da and 97182 Da. Observed mass: 97086 and 97190 Da. **E |** LC-MS analysis of Fab$_{PD-1}$-Tet-N$_3$ **4**. Expected mass: 48820 Da and 48959 Da. Observed mass: 48818 Da and 48957 Da. **F |** LC-MS analysis of Fab$_{CD3}$-Fab$_{HER2}$-Fab$_{PD-1}$-Biotin CiTE **27**. Expected mass: 146610 Da, 146749 Da and 146858 Da. Observed mass: 146618 Da, 146758 Da and 146861 Da. **G |** SDS-PAGE analysis of Fab$_{CD3}$-Fab$_{HER2}$-Fab$_{PD-1}$-Biotin CiTE **27**. **Lane 1:** Ladder. **Lane 2:** Purified Fab$_{CD3}$-Fab$_{HER2}$-Fab$_{PD-1}$-Biotin CiTE **27**. **Lane 3:** Left over bsAb (Fab$_{CD3}$-Fab$_{HER2}$-BCN **29**) after SEC. **Lane 4:** Left over Fab (Fab$_{PD-1}$-Tet-N$_3$ **4**) after SEC. **Lane 5:** Crude Fab$_{CD3}$-Fab$_{HER2}$-Fab$_{PD-1}$-Biotin CiTE **27** formation reaction. **H |** UV trace of SEC purification of Fab$_{CD3}$-Fab$_{HER2}$-N$_3$ **28**. **I |** UV trace of SEC purification of Fab$_{CD3}$-Fab$_{HER2}$-Fab$_{PD-1}$-Biotin CiTE **27**.

With the CiTE constructs prepared, their biological activity was evaluated. Initially, the binding of Fab_{HER2}-Fab_{CD3}-Sia-Biotin CiTE **26** to $HER2^+$ cancer cells (SKBR3, HCC1954, BT-20) was measured *via* flow cytometry and shown to be not significantly different from the binding of Fab_{HER2}-Fab_{CD3}-Biotin BiTE **8** to these cells (Figure 4/B). Next the binding assay was repeated on T cells, and here it was shown that the CD3-binding of CiTE **26** was significantly lower than that of BiTE **8** (Figure 4/C). We postulate that this may be due to the placement of the Fab_{CD3} moiety as it is sandwiched between the other two protein components. This decreased binding is however not necessarily a drawback – in fact, weaker binding to T cells compared to $HER2^+$ target cells could lead to better tumour-specificity and localization, and thus less systemic immune activation, lowering the risk of associated side-effects such as cytokine release syndrome.[28] It was thus established that the two Fab components of CiTE **26** retained their biological activity (as it pertains to binding), so next the activity of the sialidase enzyme component was investigated. T cells or PBMCs were incubated with CiTE **26** and BiTE **8** and the cell-surface sialic acid content was measured. While BiTE **8** as expected, exhibited no sialidase activity (as it lacks the enzyme), CiTE **26** showed significant desialylation, with activity on T cells being more than an order of magnitude higher than off-target desialylation on other PBMCs (not expressing CD3, Figure 4/D,E). It is worth noting that visualization of the binding of CiTE **26** and BiTE **8** was carried out by incubation with a streptavidin Alexa Fluor™ 647 conjugate – thus also confirming that the biotin molecule attached to the constructs retained its binding to streptavidin, and showing why the capacity of the method for functionalization of these protein–protein constructs is beneficial. The desialylation of breast cancer cell lines (HCC-1954, BT-20, MDA-MB-468 and SKBR3) by CiTE **26** was then investigated (Figure 4/F). BiTE **8** again exhibited no activity, while desialylation by CiTE **26** was dependent on HER2 expression, as $HER2^{hi}$ cells (HCC-1954 and SKBR3) were desialylated at lower concentrations than $HER2^{lo}$ cells (BT-20, MDA-MB-468). The components of CiTE **26** (Fab_{HER2}, Fab_{CD3}, ST sialidase) thus all retained their relevant biological activity despite the numerous enzymatic and chemical transformations carried out during construct-assembly.

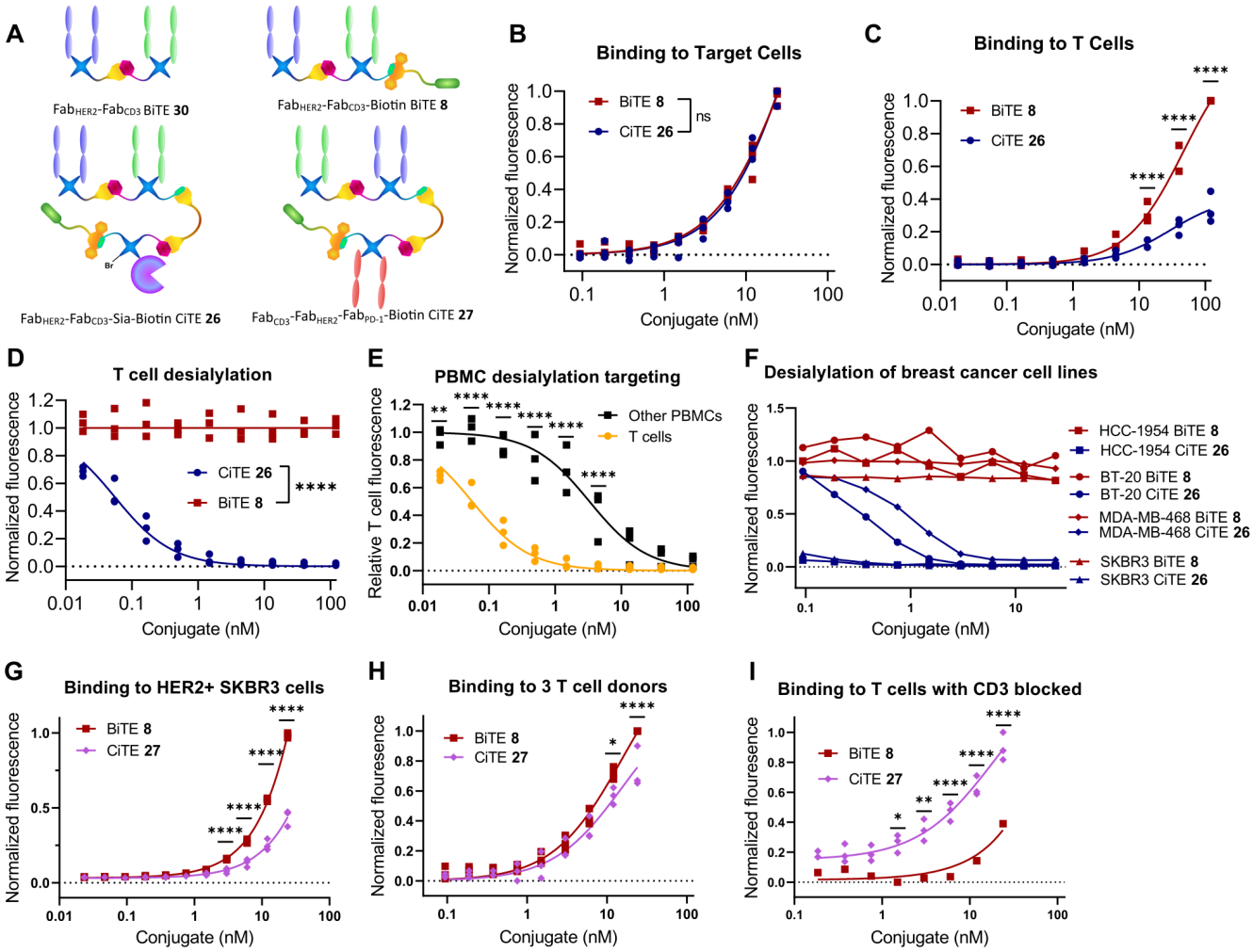

Figure 4 **| Biological testing of CiTE constructs 26 and 27. A |** Structures of constructs used in assay. **B |** Binding of Fab$_{HER2}$-Fab$_{CD3}$-Sia-Biotin CiTE **26** and Fab$_{HER2}$-Fab$_{CD3}$-Biotin BiTE **8** to HER2$^+$ cancer cell lines (SKBR3, HCC1954, BT-20) detected by flow cytometry, normalized to maximum binding. **C |** Binding of Fab$_{HER2}$-Fab$_{CD3}$-Sia-Biotin CiTE **26** and Fab$_{HER2}$-Fab$_{CD3}$-Biotin BiTE **8** to T cells from three donors detected by flow cytometry, normalized to maximum binding for each donor. **D |** Desialylation of T cells from three donors by Fab$_{HER2}$-Fab$_{CD3}$-Sia-Biotin CiTE **26** and Fab$_{HER2}$-Fab$_{CD3}$-Biotin BiTE **8**, normalized to untreated. **E |** Desialylation of T cells and PBMCs from three donors by Fab$_{HER2}$-Fab$_{CD3}$-Sia-Biotin CiTE **26**, normalized to untreated. **F |** Desialylation of cancer cells by Fab$_{HER2}$-Fab$_{CD3}$-Sia-Biotin CiTE **26**, normalized to untreated. **G |** Binding of Fab$_{CD3}$-Fab$_{HER2}$-Fab$_{PD-1}$-Biotin CiTE **27** and Fab$_{HER2}$-Fab$_{CD3}$-Biotin BiTE **8** to the HER2$^+$ SKBR3 cancer cell line detected by flow cytometry, normalized to maximum binding. **H |** Binding of Fab$_{CD3}$-Fab$_{HER2}$-Fab$_{PD-1}$-Biotin CiTE **27** and Fab$_{HER2}$-Fab$_{CD3}$-Biotin BiTE **8** to T cells from three donors detected by flow cytometry, normalized to maximum binding for each donor. **I |** Binding of Fab$_{CD3}$-Fab$_{HER2}$-Fab$_{PD-1}$-Biotin CiTE **27** and Fab$_{HER2}$-Fab$_{CD3}$-Biotin BiTE **8** to T cells from one donor, after CD3 blockade, detected by flow cytometry, normalized to maximum binding. **|** Data represented as individual datapoints, from three replicates (except in **F** and for BiTE **8** binding in **I** which are single datapoints without replicates). Statistical analysis carried out with two-way ANOVA followed by post-hoc Šídák's multiple comparisons test with multiplicity-adjusted P values with $\alpha = 0.05$. *P < 0.05, **P < 0.01, ***P < 0.001, ****P <0.0001. For **A** and **C,** the differences were not significant, and significant (****), at all concentrations, respectively. Curves fitted with non-linear regression with the following models: One-site – Specific binding: **B**, **C**, **H**. [Inhibitor] vs response (three parameters): **D**, **E**. [Agonist] vs response (three parameters): **G, I**.

This testing of components was then carried out on Fab_{CD3}-Fab_{HER2}-Fab_{PD-1}-Biotin CiTE **27**. While CiTE **27** showed binding to $HER2^+$ target cells (SKBR3), it was significantly weaker than that of Fab_{HER2}-Fab_{CD3}-Biotin BiTE **8**, corroborating the theory that the Fab sandwiched in the middle of the construct has lower binding strength – presumably due to the steric hindrance of the other two proteins on either side of it (Figure 4/G). Certainly, weaker target-binding is not desirable in this case, thus in the future a Fab_{HER2}-Fab_{CD3}-Fab_{PD-1}-Biotin CiTE would be a better candidate, with higher HER2-binding but the aforementioned lower (and beneficial) CD3-binding. Additionally, a Fab_{PD-L1} moiety would also be a more suitable way of targeting the PD-1/PD-L1 checkpoint as PD-L1 is expressed on target cells while PD-1 on effector cells – and ideally effector cell-binding would only occur in the tumour environment. Unfortunately, our efforts to obtain clean PD-L1 Fab were unsuccessful, which is why Fab_{PD-1} was our protein of choice. The binding of CiTE **27** to T cells was also compared to that of BiTE **8** and it was found that CiTE **27** bound T cells significantly weaker at higher concentrations compared to BiTE **8** (Figure 4/H). However, this decrease in T cell binding was clearly less pronounced than in the case of CiTE **26**. This increased T cell binding of CiTE **27** compared to CiTE **26** may have been due to PD-1 binding, or the change in connectivity (Fab_{CD3} now being on the outside of the construct rather than in the middle), or a combination of both. Indeed, to investigate the PD-1 binding of CiTE **27**, T cells were pre-incubated with anti-CD3 mAb, followed by incubation with varying concentration of CiTE **27** or BiTE **8** (Figure 4/I). The binding of BiTE **8** clearly decreased comparatively and was found to be significantly lower than CiTE **27** under these conditions, suggesting that Fab_{CD3}-Fab_{HER2}-Fab_{PD-1}-Biotin CiTE **27** was indeed capable of binding to PD-1. Again, all binding studies here were carried out with the aid of a dye-tagged streptavidin, showing that the biotin molecule attached to CiTE **27** provided an important advantage for ease of analysis. The components of CiTE **27** (Fab_{HER2}, Fab_{CD3}, and Fab_{PD-1}) thus also retained their binding activity, at least to an extent.

Finally, a cell-kill assay was carried out to observe whether any efficacy-increase can be attributed to the CiTE molecules compared to a conventional BiTE. Here a non-biotinylated Fab_{HER2}-Fab_{CD3} BiTE **30** (see ESI for details on synthesis) was used to conserve biotinylated Fab_{HER2}-Fab_{CD3}-Biotin BiTE **8** for studies where the biotin would be important for the visualization of binding. $HER2^+$ MDA-MB-231 cells were either untreated or incubated with IFN-γ to induce PD-L1 expression. They were then incubated with a range of concentrations of Fab_{HER2}-Fab_{CD3} BiTE **30**, Fab_{HER2}-Fab_{CD3}-Sia-Biotin CiTE **26**, or Fab_{CD3}-Fab_{HER2}-Fab_{PD-1}-Biotin CiTE **27**. In the case of both IFN-γ-treated and untreated cells both CiTEs as a trend showed greater cytotoxicity than CiTE **27** between the concentrations of 0.01 – 1 nM (Figure 5/B,C). Another general trend was the higher cytotoxicity observed in the case of IFN-γ-treated MDA-MB-231 cells.

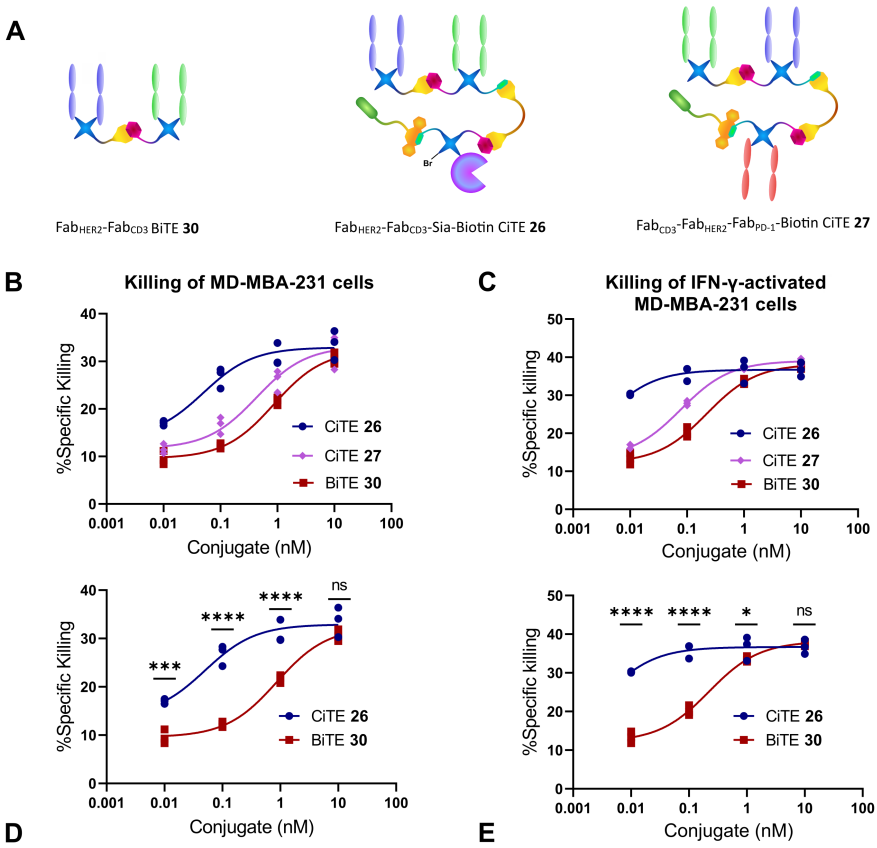

Post-hoc multiple comparisons table for BiTE vs CiTE cell-kill assay on MD-MBA-231 cells		
No induction of MD-MBA-231 PD-L1 expression		
BiTE **30** vs CiTE **26**		
Concentration	Tukey's adjusted P value	Significance
0.01 nM	0.0004	***
0.1 nM	<0.0001	****
1 nM	<0.0001	****
10 nM	0.1791	ns

Post-hoc multiple comparisons table for BiTE vs CiTE cell-kill assay on MD-MBA-231 cells		
MD-MBA-231 PD-L1 expression induced with INF-γ		
BiTE **30** vs CiTE **26**		
Concentration	Tukey's adjusted P value	Significance
0.01 nM	<0.0001	****
0.1 nM	<0.0001	****
1 nM	0.0333	*
10 nM	0.7435	ns

Figure 5 **| Cytotoxicity assay of Fab$_{HER2}$-Fab$_{CD3}$-Sia-Biotin CiTE 26 and Fab$_{CD3}$-Fab$_{HER2}$-Fab$_{PD-1}$-Biotin CiTE 27. A |** Structures of constructs used in assay. **B |** Cytotoxicity assay of Fab$_{HER2}$-Fab$_{CD3}$-Sia-Biotin CiTE **26** and Fab$_{CD3}$-Fab$_{HER2}$-Fab$_{PD-1}$-Biotin CiTE **27**. MDA-MB-231 cells were co-cultured with T cells (E:T ratio of 2:1) and treated with 0.01 – 10 nM of CiTE **26**, CiTE **27** or BiTE **30**. MDA-MB-231 viability was assessed 24 h following treatment *via* LDH assay. **C |** Cytotoxicity assay of Fab$_{HER2}$-Fab$_{CD3}$-Sia-Biotin CiTE **26** and Fab$_{CD3}$-Fab$_{HER2}$-Fab$_{PD-1}$-Biotin CiTE **27**. MDA-MB-231 cells, pre-incubated with IFN-γ to induce PD-L1 expression, were co-cultured with T cells (E:T ratio of 2:1) and treated with 0.01 – 10 nM of CiTE **26**, CiTE **27** or BiTE **30**. MDA-MB-231 viability was assessed 24 h following treatment *via* LDH assay. **D |** Comparison of cytotoxicity of CiTE **26** and BiTE **30** on MDA-MB-231 cells. Statistical analysis carried out with two-way ANOVA followed by post-hoc Tukey's multiple comparisons test with multiplicity-adjusted P values with $\alpha = 0.05$. **E |** Comparison of cytotoxicity of CiTE **26** and BiTE **30**, with IFN-γ-activated MDA-MB-231 cells. Statistical analysis carried out with two-way ANOVA followed by post-hoc Tukey's multiple comparisons test with multiplicity-adjusted P values with $\alpha = 0.05$. *P < 0.05, **P < 0.01, ***P < 0.001, ****P <0.0001. Data represented as individual datapoints, from three replicates. Curves fitted with non-linear regression with the following model: [Agonist] vs response (three parameters). See ESI for ANOVA table and comparisons between CiTE **27** and BiTE **30**, and CiTE **26** and CiTE **27**.

PD-1 blocking CiTE **27** was slightly more potent at lower concentrations than BiTE **30**, especially when the MDA-MB-231 cells were treated with IFN-γ to induce PD-L1 expression (see ESI). However, sialidase-containing CiTE **26** was significantly more active at lower concentrations than either CiTE **27** or BiTE **30**, suggesting that under these conditions desialylation is highly synergistic with T cell engagement, and more so than PD-1/PD-L1 checkpoint blockade (Figure 5/D,E, and see ESI for additional comparisons). The catalytic activity of sialidase enzyme contrasted with the stoichiometric nature of PD-1 blockade could perhaps play a role in how active CiTE **26** was at low concentrations compared to CiTE **27.** Indeed, the cancer cell and T cell desialylation data discussed previously (Figure 4/D,F) suggests that all sialic acid is removed by between 0.1 nM and 1 nM CiTE **26**, facilitating T cell-mediated cytotoxicity.

Conclusion and Outlook

In summary, a first-in-class method was developed for the chemical generation of functionalized three-protein constructs. Checkpoint-inhibitory T cell engager (CiTE) molecules with either an ST sialidase enzyme for removal of immuno-suppressive sialic acid glycans from target and effector cells,[25] or an anti-PD-1 Fab checkpoint inhibitor[19] attached were synthesized along with relevant controls. The syntheses were carried out *via* tetrazine–BCN SPIEDAC click chemistry for protein–protein conjugation, and each CiTE had a biotin small molecule also conjugated *via* SPAAC for imaging and/or purification. These CiTE molecules were then tested for their biological activity. Due to the modularity of this method, showcased here, it could be applied to the generation of a wide variety of three-protein constructs. BiTEs could be conjugated to different checkpoint inhibitors (e.g., CTLA-4, ICOS) or cytokines (e.g., IL2),[29] the selectivity of the construct could be improved by targeting two separate tumour-associated receptors in addition to CD3, or target-independent immune-activators could be developed to re-activate exhausted T cells regardless of cancer indication.[26] The method has the added flexibility of an inherent handle for the attachment of small molecules, e.g., biotin, fluorophores, cytotoxins, half-life extenders or activity-masking moieties.[30,31] The strategy also, to some extent, enables control over the binding-profile of the constructs, as it seems that the Fab moiety sandwiched in the middle of the three-protein species has reduced ability to bind its target, presumably due to steric hindrance. This could be exploited to minimize unwanted binding, and thus potentially reduce side effects. The method is also rapid (the conjugates can be prepared starting from mAbs within a 5-7 day timescale) and modular (works with most mAbs and cysteine-mutant proteins). It could thus be very useful in hit-identification, where a large number of constructs with various protein-combinations are generated from a pool of biomacromolecules, e.g., in a 96-well plate. These crude constructs could then be screened for biological activity and the most promising hits scaled up for further testing. The scalability and developability of this strategy should, however, be investigated as based on current information it is hard to judge whether it would be feasible

to make the shift to large-scale industrial production. That being said, we do not see any inherent reason it could not, provided the process can be streamlined to minimize protein-loss during purification steps, as the chemical reactions themselves all proceed with excellent conversions.

The generated constructs, Fab_{HER2}-Fab_{CD20}-Sia-Biotin **20**, Fab_{HER2}-Fab_{CD3}-Sia-Biotin CiTE **26** and Fab_{CD3}-Fab_{HER2}-$Fab_{PD\text{-}1}$-Biotin CiTE **27** along with simpler two-protein constructs had their biological activities investigated. The constituent parts were shown to retain their biological function (although binding was impaired in some cases). The CiTEs were then shown to be significantly more effective than the corresponding BiTE **30** at killing $HER2^+$ cells in the presence of T cells. While the increase in efficacy of PD-1 blocking CiTE **27** was perhaps not astounding in its magnitude, there was significant benefit in adding the checkpoint inhibitory modality to a BiTE scaffold even under these relatively unoptimized conditions. The sialidase containing CiTE **26** however had robustly increased cytotoxic activity (by about an order of magnitude) at lower concentrations than BiTE **30.** Carrying out more in-depth biological assays (including *in vivo* assays and testing different $HER2^+$ cancer cells lines) was beyond the scope of this chemistry-focused project, but since other groups have demonstrated the synergy between checkpoint inhibition and T cell engagement,[19] we believe this exciting angle of immunomodulation should be explored further, especially as this work goes on to show that sialic-acid removal is strongly synergistic with BiTE treatment *in vitro*. Furthermore, we hope we have provided a method and proof-of-concept for the generation of such three-protein constructs to enable further innovation in the field. We also hope we have demonstrated the power of bioorthogonal chemical strategies for protein–protein conjugation, as while this area of research has been gaining momentum recently,[5,6] there is much untapped potential that is still waiting to be uncovered.

Acknowledgments

We gratefully acknowledge the Wellcome Trust for funding P.S., a grant from the National Institutes of Health (NIH R01 CA227942 to C.R.B.), the Leverhulme Trust (RPG-2020-010) for funding C.B. and the EU's Horizon 2020 programme under Marie-Curie grant agreement 675007 for funding J.N. We also acknowledge Dr Kersti Karu of the UCL Chemistry Mass Spectrometry (MS) Facility, Dr Abil Aliev of the UCL NMR service as well as Dr Nikos Pinotsis of the ISMB Biophysics Centre. As M.G. and M.R. contributed equally to this work, they are permitted to list their names as second on the author list on any C.V. or grant and fellowship application, etc. Their names were merely listed in this order alphabetically. This research was funded in part by the Wellcome Trust [Grant number: 175282, 214941/Z/18/Z]. For the purpose of Open Access, the author has applied a CC BY public copyright licence to any Author Accepted Manuscript version arising from this submission.

Authors' contributions

P.S. prepared the antibody fragments. P.S., C.B. and J.N. synthesized the small molecules. P.S. generated the protein constructs. P.S. carried out the SEC purifications. P.S. analysed the protein constructs by LC-MS and SDS-PAGE. M.G. and M.R. performed the biology experiments. P.S. and M.G. carried out the statistical analysis. P.S., M.G., C.R.B. and V.C. devised the study. All authors contributed to the writing of this manuscript. All authors read and approved the final manuscript.

Competing interests

M.A.G. and C.R.B. are inventors of the patent filed by Stanford University (international publication number WO2018006034A1) titled 'Conjugates for targeted cell-surface editing' published on January 4, 2018 and licensed by Palleon Pharmaceuticals on 06/27/2017. C.R.B. is a cofounder and Scientific Advisory Board member of Palleon Pharmaceuticals, Enable Bioscience, Redwood Biosciences (a subsidiary of Catalent) and InterVenn Biosciences, and a member of the Board of Directors of Eli Lilly & Company. V.C is a director of the spin-out ThioLogics, but there are no competing financial interests to declare.

References

1. Gera, N. The evolution of bispecific antibodies. *Expert Opin. Biol. Ther.* **22**, 945–949 (2022).

2. Budde, L. E. *et al.* Safety and efficacy of mosunetuzumab , a bispecific antibody , in patients with relapsed or refractory follicular lymphoma : a single-arm , multicentre , phase 2 study. *Lancet Oncol.* **23**, 1055–1065 (2022).

3. Husain, B. & Ellerman, D. Expanding the Boundaries of Biotherapeutics with Bispecific Antibodies.

BioDrugs **32**, 441–464 (2018).

4. Thoreau, F. & Chudasama, V. Enabling the next steps in cancer immunotherapy: from antibody-based bispecifics to multispecifics, with an evolving role for bioconjugation chemistry. *RSC Chem. Biol.* **3**, 140–169 (2022).

5. Szijj, P. & Chudasama, V. The renaissance of chemically generated bispecific antibodies. *Nat. Rev. Chem.* **5**, 78–92 (2021).

6. Taylor, R. J., Geeson, M. B., Journeaux, T. & Bernardes, G. J. L. Chemical and Enzymatic Methods for Post-Translational Protein − Protein Conjugation. *J. Am. Chem. Soc.* **144**, 14404–14419 (2022).

7. Moura, A., Savageau, M. A. & Alves, R. Relative Amino Acid Composition Signatures of Organisms and Environments. *PLoS One* **8**, e77319 (2013).

8. Khalili, H. *et al.* Fab-PEG-Fab as a potential antibody mimetic. *Bioconjugate Chem.* **24**, 1870–1882 (2013).

9. Hull, E. A. *et al.* Homogeneous bispecifics by disulfide bridging. *Bioconjugate Chem.* **25**, 1395–1401 (2014).

10. Forte, N. *et al.* Tuning the Hydrolytic Stability of Next Generation Maleimide Cross-Linkers Enables Access to Albumin-Antibody Fragment Conjugates and tri-scFvs. *Bioconjugate Chem.* **29**, 486–492 (2018).

11. Patterson, J. T. *et al.* PSMA-targeted bispecific Fab conjugates that engage T cells. *Bioorganic Med. Chem. Lett.* **27**, 5490–5495 (2017).

12. Patterson, J. T. *et al.* Chemically generated IgG2 bispecific antibodies through disulfide bridging. *Bioorganic Med. Chem. Lett.* **27**, 3647–3652 (2017).

13. Maruani, A. *et al.* A Plug-and-Play Approach for the de Novo Generation of Dually Functionalized Bispecifics. *Bioconjugate Chem.* **31**, 520–529 (2020).

14. Lee, M. T. W., Maruani, A. & Chudasama, V. The use of 3,6-pyridazinediones in organic synthesis and chemical biology. *J. Chem. Res.* **40**, 1–9 (2016).

15. Bahou, C. *et al.* Highly homogeneous antibody modification through optimisation of the synthesis and conjugation of functionalised dibromopyridazinediones. *Org. Biomol. Chem.* **16**, 1359–1366 (2018).

16. Robinson, E. *et al.* Pyridazinediones deliver potent, stable, targeted and efficacious antibody-drug

conjugates (ADCs) with a controlled loading of 4 drugs per antibody. *RSC Adv.* **7**, 9073–9077 (2017).

17. Lee, M. T. W., Maruani, A., Baker, J. R., Caddick, S. & Chudasama, V. Next-generation disulfide stapling: Reduction and functional re-bridging all in one. *Chem. Sci.* **7**, 799–802 (2016).

18. Maruani, A. *et al.* A mild TCEP-based *para* -azidobenzyl cleavage strategy to transform reversible cysteine thiol labelling reagents into irreversible conjugates. *Chem. Commun.* **51**, 5279–5282 (2015).

19. Herrmann, M. *et al.* Bifunctional PD-1 3 aCD3 3 aCD33 fusion protein reverses adaptive immune escape in acute myeloid leukemia. *Blood* **132**, 2484–2494 (2018).

20. Rader, C. Bispecific antibodies in cancer immunotherapy. *Curr. Opin. Biotechnol.* **65**, 9–16 (2020).

21. Bukhari, A. & Lee, S. T. Blinatumomab: a novel therapy for the treatment of non-Hodgkin's lymphoma. *Expert Rev. Hematol.* **12**, 909–918 (2019).

22. Krupka, C. *et al.* Blockade of the PD-1/PD-L1 axis augments lysis of AML cells by the CD33/CD3 BiTE antibody construct AMG 330: Reversing a T-cell-induced immune escape mechanism. *Leukemia* **30**, 484–491 (2016).

23. Roskopf, C. C. *et al.* T cell-recruiting triplebody 19-3-19 mediates serial lysis of malignant B-lymphoid cells by a single T cell. *Oncotarget* **5**, 6466–6483 (2014).

24. Xiao, H., Woods, E. C., Vukojicic, P. & Bertozzi, C. R. Precision glycocalyx editing as a strategy for cancer immunotherapy. *Proc. Natl. Acad. Sci. U. S. A.* **113**, 10304–10309 (2016).

25. Gray, M. A. *et al.* Targeted glycan degradation potentiates the anticancer immune response in vivo. *Nat. Chem. Biol.* **16**, 1376–1384 (2020).

26. Edgar, L. J. *et al.* Sialic Acid Ligands of CD28 Suppress Costimulation of T Cells. *ACS Cent. Sci.* **7**, 1508–1515 (2021).

27. Baalmann, M. *et al.* A Bioorthogonal Click Chemistry Toolbox for Targeted Synthesis of Branched and Well-Defined Protein–Protein Conjugates. *Angew. Chem. Int. Ed.* **59**, 12885–12893 (2020).

28. Strohl, W. R. & Naso, M. Bispecific t-cell redirection versus chimeric antigen receptor (car)-t cells as approaches to kill cancer cells. *Antibodies* **8**, 41 (2019).

29. Neri, D. Antibody–cytokine fusions: Versatile products for the modulation of anticancer immunity. *Cancer Immunol. Res.* **7**, 348–354 (2019).

30. Autio, K. A., Boni, V., Humphrey, R. W. & Naing, A. Probody therapeutics: An emerging class of therapies designed to enhance on-target effects with reduced off-tumor toxicity for use in immuno-oncology. *Clin. Cancer Res.* **26**, 984–989 (2020).

31. Lucchi, R., Bentanachs, J. & Oller-Salvia, B. The Masking Game: Design of Activatable Antibodies and Mimetics for Selective Therapeutics and Cell Control. *ACS Cent. Sci.* **7**, 724–738 (2021).